IN-PLANE BEHAVIOUR OF WEB-TAPERED BEAMS

NICHOLAS TRAHAIR
PETER ANSOURIAN

RESEARCH REPORT R956
OCTOBER 2015

ISSN 1833-2781

SCHOOL OF CIVIL ENGINEERING

THE UNIVERSITY OF SYDNEY

THE UNIVERSITY OF SYDNEY

SCHOOL OF CIVIL ENGINEERING

IN-PLANE BEHAVIOUR OF WEB-TAPERED BEAMS

RESEARCH REPORT R956

NS TRAHAIR AND P ANSOURIAN

OCTOBER 2015

ISSN 1833-2781

Copyright Notice

School of Civil Engineering, Research Report R956
NS Trahair and P Ansourian
October 2015

ISSN 1833-2781

Published by:
School of Civil Engineering
The University of Sydney
Sydney NSW 2006
Australia

This report and other Research Reports published by the School of Civil Engineering are available at http://sydney.edu.au/civil

ABSTRACT

Shear stress distributions in tapered web I-beams are incorrectly predicted by the conventional beam analysis method used for uniform beams. More accurate predictions are obtained by adopting the finding for wedges that the normal stress trajectories are radial instead of parallel.

The shear stress distributions in web-tapered I-beams are influenced by the vertical components of the inclined flange forces (which are zero in uniform beams), as well as by the normal stress gradients in the flanges. The net web shear equal to the difference between the external shear and the vertical components of the inclined flange forces is resisted by the resultant of the vertical components of the normal stresses and the circumferential shear stresses.

The circumferential shear stresses have linear components due to axial force and parabolic components due to moment and shear. The magnitudes of these stresses are controlled by the normal stress gradients at the flange-web junctions and by the requirement that the web shear resistance must equal the net web shear force.

KEYWORDS

Bending, deflections, elasticity, force, I-beam, normal stress, shear, shear stress, tapered web, edge

TABLE OF CONTENTS

1. INTRODUCTION

The in-plane behaviour of tapered I-beams (Fig. 1) is rarely treated in textbooks, but designers commonly assume that they behave in the same way as uniform beams. While this may be satisfactory for the bending deflections and the normal stresses, it may lead to incorrect shear stress distributions.

In uniform I-section beams, the normal stresses due to moments and axial forces are parallel to the centroidal axis, while the shear forces are resisted solely by shear stresses in the web [1]. However, in web-tapered beams, the flanges are inclined to the centroidal axis, as are the flange normal stresses, and so the stress trajectories are inclined to the centroidal axis. In addition, the inclined flange forces have components transverse to the centroidal axis, which may participate in resisting the shear forces.

In this paper, the distributions of the normal and shear stresses in web-tapered I-beams are investigated. First, the known stress distributions in tapered plate wedges (Fig. 2) are reviewed, because of the similarity of tapered wedges to the webs of tapered I-beams. These suggest that the normal stresses in web-tapered I-beams might be assumed to be radial. This assumption is then used to analyse the distributions of normal and shear stresses. Finally, the predicted stress distributions are compared with those obtained from a more rigorous finite element program [2] which incorporates the two-dimensional membrane behaviour of the flange and web plates of which the tapered beams are composed.

2. PLATE WEDGES

The stresses in wedges (Fig. 2) have been reported in [3]. For a wedges of included angle 2α with an end compression load $-N$ acting along the axis, the stress distribution at a distance r from the apex of the wedge is purely radial (Fig. 3a), with zero circumferential normal stresses σ_θ and shear stresses $\tau_{r\theta}$. The radial stresses

$$\sigma_r = -\frac{2N\cos\theta}{r(2\alpha + \sin 2\alpha)} \tag{1}$$

vary with the angle θ from the axis, but are nearly uniform for wedges with small taper angles α. The stress trajectories are clearly radial along the lines θ = constant, which are also principal stress contours.

For wedges with end loads V acting transverse to the axis, the stress distribution is again radial (Fig. 3b), with zero circumferential normal stresses σ_θ and shear stresses $\tau_{r\theta}$ and

$$\sigma_r = -\frac{2V\sin\theta}{r(2\alpha - \sin 2\alpha)} \tag{2}$$

The variation of these stresses with the angle θ is nearly linear for small taper angles α. Again, the stress trajectories are radial along the lines θ = constant, which are also principal stress contours.

For these wedges, the end load V causes bending moments and shear forces which vary along the axis. The variation of the horizontal components of σ_r in wedges with small tapers is close to the linear variation of σ_z for moment predicted by conventional beam analysis (CBA). However, the variation of the vertical components is very different to that of CBA, for which the distribution of the shear stress τ_{yz} is parabolic with zero stresses at the top and bottom edges, and 1.5 times the average at the axis. For the wedge, the shear stress τ_{yz} variation is also parabolic, but with zero stress at the axis and 3 times the average at the top and bottom edges. The sums of the horizontal and vertical components of σ_r are equal to the moment and shear effects of the applied load.

For wedges with end moments M, the circumferential normal stresses σ_θ are again zero, but the radial stresses are accompanied by shear stresses (Fig. 3c). The radial stresses are

$$\sigma_r = -\frac{4M\sin 2\theta}{2r^2(\sin 2\alpha - 2\alpha\cos 2\alpha)} \tag{3}$$

and the shear stresses are

$$\tau_{r\theta} = \frac{2M(\cos 2\theta - \cos 2\alpha)}{2r^2(\sin 2\alpha - 2\alpha\cos 2\alpha)} \tag{4}$$

The variation of the horizontal components σ_z in wedges with small tapers is close to the linear variation of CBA for moment. The vertical components of the radial stresses vary from maxima at the edges to zero at the axis, and are so balanced by the vertical components of the shear stresses that there is no vertical shear resultant. Because of the presence of shear stresses, the principal stress trajectories are not quite radial.

It can be concluded that the normal stress distributions in small taper wedges are radial, and are closely approximated by CBA. However, the shear stress distributions are quite different to those predicted by CBA.

3. WEB-TAPERED BEAMS

3.1 Beams

A simply supported web-tapered beam with equal uniform flanges is shown in Fig. 1. The beam length is L = 152 mm. The cross-section dimensions are shown in Table 1.

Table 1. Cross-Section Dimensions

Dimension	Section 1	Section 2
r (mm)	101.31	177.31
b_f (mm)	31.55	31.55
b_w (mm)	29.10	72.76
t_f (mm)	3.11	3.11
t_w (mm)	2.13	2.13

3.2 Methods of Analysis

3.2.1 Tapered Beam Analysis (TBA)

The methods of linear elastic analysis (CBA) of uniform beams are well documented [1]. In summary, plane sections are assumed to remain plane and shear strains are neglected in the analysis of the bending deflections and stress concentrations at applied loads or reactions are ignored. The section properties of area A and second moment of area I_x are used to determine the longitudinal normal stresses σ caused by axial force N and bending moment M_r, which are determined from the applied loads and moments either by equilibrium for determinate beams or by analysis of the bending deflections v for indeterminate beams. In Appendix 1, CBA analysis of bending and compression is adapted to web-tapered I-beams by assuming that the normal stress trajectory inclinations vary linearly between those of the edges of the plates of which the beam is composed, as suggested by the wedge stress distributions of Fig. 3. This adapted analysis using inclined stress trajectories is referred to in this paper as tapered beam analysis (TBA).

In uniform plates, shear force V induces a parabolic distribution of transverse shear stress, from zero at the top and bottom edges to a maximum at the mid-height. It was noted above that this distribution is incorrect for tapered wedges (Fig. 3b). The similarity of tapered wedges to the webs of web-tapered I-beams suggests that the conventional analysis of the shear stresses in uniform beams requires significant modification before it can be applied to web-tapered I-beams. In Appendix 2, CBA analysis of shear is modified for web-tapered I-beams.

3.2.2 Finite Element Analysis (FEA)

For this paper, the bending and compression of tapered I- beams has been analysed (FEA) by using the finite element computer program STRAND7 [2]. This software contains a variety of plate/shell elements for the analysis of plane stress/strain/axisymmetric, and general shell structures. In the context of this paper, the QUAD4 plate/shell element has been used for the analysis of tapered web and flange problems. The element provides high accuracy for relatively coarse meshes and is well suited for the analysis of I-section beams modelled with 3 plates for the two flanges and the web, any of which can be tapered in their own plane. The element is based on conventional thin plate theory, and can tolerate skews in the range 45-135 degrees, and aspect ratios up to 4. In regions of high stress gradient, the skew should be closer to 90 degrees and the aspect ratio closer to one. The state of stress within a flange or web is one of plane stress including membrane normal and shear stresses. Local stress concentrations are captured in the neighbourhood of applied nodal forces.

3.3 Axial Compression

The web-tapered I-beam shown in Fig. 4a has equal and opposite axial forces $-N$ which induce compressive normal stresses in the beam. The stresses within this beam have been determined by TBA using inclined stress trajectories. The inclined (radial) web stresses σ_r are constant across any cross-section and the self-equilibrating tangential shear stresses $\tau_{r\theta}$ vary linearly, as shown diagrammatically in Fig. 4a.

The radial and circumferential stresses may be converted to longitudinal normal stresses σ_z and transverse shear stresses τ_{zy} by assuming that tangential normal stresses (σ_θ) are zero, whence [3]

$$\begin{aligned} \sigma_z &= \sigma_r \cos^2\theta - 2\tau_{r\theta}\sin\theta\cos\theta \\ \tau_{zy} &= \tau_{r\theta}(\cos^2\theta - \sin^2\theta) - \sigma_r \sin\theta\cos\theta \end{aligned} \tag{5}$$

The values of the mid-span stresses at the centroid and bottom flange-web junction ($\theta = \alpha$) are shown in Table 2.

The radial stresses σ_r are equivalent to a set of almost constant longitudinal normal stresses σ_z and a self-equilibrating set of linear shear stresses $\theta\sigma_r$. The shear stresses τ_{zy} are approximated by

$$\tau_{zy} = \tau_{r\theta} + \theta\sigma_r \tag{6}$$

These shear stresses differ from the zero stresses predicted by CBA.

The vertical components of the shear stresses satisfy the equation

$$V = V_f + \int_{-\alpha}^{\alpha} \tau_{r\theta} r t_w d\theta + \int_{-\alpha}^{\alpha} \theta\sigma_\theta r t_w d\theta \tag{7}$$

in which V is the total shear and V_f is the sum of the vertical components of the flange normal forces

$$V_f = \alpha b_f t_f \{(\sigma_r)_\alpha b - (\sigma_r)_{-\alpha}\} \tag{8}$$

In this case, $V = V_f$=0.

The stresses within this beam have also been determined by FEA [2]. The length of this beam is very short, so that significant shear effects and end stress concentrations may occur. The values of the mid-span stresses at the bottom flange-web junction are close to those determined by TBA, as shown in Table 2. The small discrepancies may be due to the assumption made in Appendices 1 and 2 that θ is small, and due to the effects of stress concentrations on the FEA results.

Table 2 Comparison of Mid-Span Stresses

Figure	Loading	Analysis	σ_{zc} (N/mm^2)	$\sigma_{z\alpha}$ (N/mm^2)	τ_{yzc} (N/mm^2)	$\tau_{yz\alpha}$ (N/mm^2)
4a	N = –10^4 N	TBA	–32.8	–33.0	0	–1.7
		FEA	–33.5	–33.1	0	–1.6
4b	V = –10^4 N	TBA	0	297	6.0	30.5
		FEA	0	297	6.4	28.0
4c	M = 10^6 Nmm	TBA	0	180	–54.5	–24.9
		FEA	0	177	–52.7	–25.0

3.4 Shear

The beam shown in Fig. 4b has a shear force V acting at the intersection of the flanges and an equilibrating moment V (r_0+L) and shear force V at the right-hand end. The stresses within this beam have been determined by TBA using inclined stress trajectories. The inclined (radial) stresses σ_r vary linearly across any cross-section and the self-equilibrating tangential shear stresses $\tau_{r\theta}$ vary parabolically, as shown in Fig. 4b. The values of the mid-span stresses at the centroid and bottom flange-web junction are shown in Table 2.

The radial stresses σ_r are equivalent to a set of linear longitudinal normal stresses σ_z and a set of parabolic shear stresses $\theta\sigma_r$. The parabolic transverse shear stresses τ_{zy} (Equation 6) differ significantly from the almost constant stresses predicted by CBA, not only in their distribution, but also in their magnitudes. They are greatly reduced by the reduction of the net web shear $V - V_f$ caused by the vertical components V_f of the flange forces.

The stresses within this beam have also been determined by FEA [2]. The values of the mid-span stresses at the centroid and bottom flange-web junction are close to those determined by TBA, as shown in Table 2.

3.5 Moment

The beam shown in Fig. 4c has equal and opposite end moments M. The stresses within this beam have been determined by TBA using inclined stress trajectories. The inclined (radial) stresses σ_r vary linearly across any cross-section and the tangential shear stresses $\tau_{r\theta}$ are nearly constant, as shown in Fig. 4b. The values of the mid-span stresses at the centroid and bottom flange-web junction are shown in Table 2.

The radial stresses σ_r are equivalent to a set of linear longitudinal normal stresses σ_z and a set of parabolic shear stresses $\theta\sigma_r$. The parabolic transverse shear stresses τ_{zy} (Equation 6) differ significantly from the zero stresses predicted by CBA. These stresses balance the vertical components V_f of the flange forces so that the net shear force on the section is zero

The stresses within this beam have also been determined by FEA [2]. The values of the mid-span stresses at the centroid and bottom flange-web junction are close to those determined by TBA, as shown in Table 2.

4 DISCUSSION AND CONCLUSIONS

The normal stresses in wedges [3] are solely radial (σ_θ = 0). The similarity of wedges to the webs of web-tapered I-beams suggests that web normal stresses are also solely radial. Analysis (TBA) based on this assumption leads to normal stress magnitudes and deflections which are the same as those predicted by conventional beam analysis (CBA) based on the assumption that the normal stress trajectories are parallel to the centroidal axis. However, the shear stress distributions in web-tapered I-beams predicted by CBA are markedly different from those of TBA, just as they are for wedges [3].

The shear stress distributions in web-tapered I-beams are influenced by the vertical components of the inclined flange forces (which are zero in uniform beams), as well as by the normal stress gradients in the flanges. The net web shear equal to the difference between the external shear V and the vertical components of the inclined flange forces V_f is resisted by the resultant of the vertical components $\theta_{\sigma r}$ of the normal stresses and the circumferential shear stresses $\tau_{r\theta}$ (Equation 7).

The circumferential shear stresses $\tau_{r\theta}$ have linear components due to axial force and parabolic components due to moment and shear. The magnitudes of these stresses are controlled by the normal stress gradients at the flange-web junctions and by the requirement that the web shear resistance must equal the net web shear force.

The shear stresses determined in this manner (TBA) are in reasonable agreement with the more accurate stresses determined by finite element analysis (FEA).

5 REFERENCES

[1] Trahair, NS, Bradford, MA, Nethercot, DA, and Gardner, L, *The Behaviour and Design of Steel Structures to EC3*, 4th ed., Taylor and Francis, London, 2008.

[2] Strand7 Pty Ltd, STRAND7, Sydney, 2015.

[3] Timoshenko, SP and Goodier, JN, *Theory of Elasticity*, 2nd ed., McGraw-Hill, New York, 1951.

APPENDIX A. BENDING AND COMPRESSION ANALYSIS (TBA)

The bending and compression of a web-tapered I-beam is summarised in the subsections below for the section properties, the element model, the deflections and rotations, and the normal strains and stresses.

A.1 Section Properties

The doubly symmetric I-section shown in Fig. 1a has top and bottom flange and web widths b_f, b_f, and b_w and thicknesses t_f, t_f, and t_w, respectively. The element shown in Fig.1b has constant thicknesses and flange widths, but may have linearly tapered web widths.

The area of the section is

$$A = 2b_f t_f + b_w t_w \tag{A.1}$$

and the major axis second moment of area is

$$I_x = b_f t_f b_w{}^2 / 2 + b_w^3 t_w / 12 \tag{A.2}$$

A.2 Element Model

The origin of the y, z axes is at the intersection of the flange centre lines, the z axis of the element is the longitudinal axis of symmetry, and the y axis is perpendicular, as shown in Fig. 1b. The position of any point P(y,z) may also be defined by the coordinates

$$\begin{aligned} r &\approx z \\ \theta &\approx y / r \end{aligned} \tag{A.3}$$

The web edges are defined by

$$\pm\theta = \alpha = b_{w0} / 2z_0 \tag{A.4}$$

in which z_0 is the distance to the left hand end of the element and b_{w0} is the value of b_w at $z = z_0$.

The tapered element is modelled as being composed of tapered longitudinal fibres PP inclined at θ to the z axis.

A.3 Deflections and Rotations

The applied loading causes the typical cross-section of the element to displace and rotate in the yz plane. These deformations may be defined by the in-plane displacements v perpendicular to and w along the z axis, and rotations v', in which ' $\equiv d/dz \approx d/dr$. The in-plane displacements perpendicular and parallel to the z axis of a point P(y, z) are given by

$$\begin{aligned} v_P &= v \\ w_P &= w - r\theta v' \end{aligned} \tag{A.5}$$

and the displacement along the inclined fibre PP is given by

$$w_r = w_P + \theta v_P = w - r\theta v' + \theta v \tag{A.6}$$

A.4 Strains and Stresses

The normal linear strain along the inclined fibre is

$$\varepsilon_r = w_r' = w' - r\theta v'' = w' - yv'' \tag{A.7}$$

and the tensile stress is

$$\sigma_r = E\varepsilon_r \tag{A.8}$$

in which E is the Young's modulus of elasticity. After using

$$\int_A dA = A, \quad \int_A y dA = 0, \quad \int_A y^2 dA = I_x \tag{A.9}$$

the stress can be expressed as

$$\sigma_r = N / A + M_r y / I_x \tag{A.10}$$

in which the axial tension N and the bending moment M_r are given by

$$N = \int_A \sigma_r dA = EAw' \tag{A.11}$$

$$M_r = \int_A \sigma_r y dA = -EI_x v'' \tag{A.12}$$

Equations A.10 – A.12 are the same as those used in the elastic analysis of uniform beams under bending and compression (CBA). They are independent of the taper angle α.

APPENDIX B. SHEAR STRESS ANALYSIS (TBA)

Equation A.10 for the radial stress can be expressed as

$$\sigma_r = N / A + M_r r\theta / I_x \tag{B.1}$$

so that

$$\frac{\partial \sigma_r}{\partial r} = -\frac{N}{A^2}\frac{dA}{dr} + \frac{M_r \theta}{I_x}\left\{1 + \frac{r}{M_r}\frac{dM_r}{dr} - \frac{r}{I_x}\frac{dI_x}{dr}\right\} = -\frac{N}{A^2}\frac{dA}{dr} + \frac{M_r \theta k}{I_x} \tag{B.2}$$

in which

$$k = 1 + \frac{r}{M_r}\frac{dM_r}{dr} - \frac{r}{I_x}\frac{dI_x}{dr} \tag{B.3}$$

In the bottom flange ($\theta = \alpha$)

$$\frac{\partial \tau_{rx}}{\partial x} = -\left(\frac{\partial \sigma_r}{\partial r}\right)_\alpha \tag{B.4}$$

and the shear flow into the web is

$$\tau_{r\theta\alpha} t_w = b_f t_f \left(\frac{\partial \sigma_r}{\partial r}\right)_\alpha \tag{B.5}$$

in which

$$\left(\frac{\partial \sigma_r}{\partial r}\right)_\alpha = -\frac{N}{A^2}\frac{dA}{dr} + \frac{M_r \alpha k}{I_x} \tag{B.6}$$

In the web, when the tangential stress σ_θ is equal to zero, then the radial equilibrium equation is [3]

$$\frac{\partial \tau_{r\theta}}{\partial \theta} = -\left\{\sigma_r + r\frac{\partial \sigma_r}{\partial r}\right\} \tag{B.7}$$

or

$$\begin{aligned}\frac{\partial \tau_{r\theta}}{\partial \theta} &= -\left\{\frac{N}{A}\left(1 - \frac{r}{A}\frac{dA}{dr}\right) + \frac{M_r r\theta}{I_x}\left(2 + \frac{r}{M_r}\frac{dM_r}{dr} - \frac{r}{I_x}\frac{dI_x}{dr}\right)\right\} \\ &= -\left\{\frac{N}{A}\left(1 - \frac{r}{A}\frac{dA}{dr}\right) + \frac{M_r r\theta(k+1)}{I_x}\right\}\end{aligned} \tag{B.8}$$

Thus

$$\tau_{r\theta} = -\left\{\frac{N\alpha}{A}\left(1 - \frac{r}{A}\frac{dA}{dr}\right)\left(\frac{\theta}{\alpha} + C_n\right) + \frac{M_r r\alpha^2(k+1)}{I_x}\left(\frac{\theta^2}{\alpha^2} + C_m\right)\right\} \tag{B.9}$$

The constants of integration C_n, C_m can be determined by equating the expression for $\tau_{r\theta\alpha}$ obtained from Equation B.9 by setting $\theta = \alpha$ to that obtained from Equation B.5. These allow Equation B.9 to be expressed as

$$\tau_{r\theta} = \tau_{\alpha n}\theta/\alpha + \tau_{0m} + (\tau_{\alpha m} - \tau_{0m})\theta^2/\alpha^2 \tag{B.10}$$

in which

$$\tau_{\alpha n} = -\frac{N b_f t_f}{A^2 t_w}\frac{dA}{dr}$$
$$\tau_{0m} = \frac{M_r r \alpha^2 (k+1)}{I_x}\left\{1 + \frac{2 b_f t_f}{b_w t_w}\frac{k}{k+1}\right\} \quad \text{(B.11)}$$
$$\tau_{\alpha m} = \frac{M_r \alpha b_f t_f k}{t_w I_x}$$

NOTATION

A	Area of cross-section
$b_{f,,w}$	Flange width and web depth
b_{w0}	Flange width at $z = 0$
$C_{m,n}$	Constants of integration
E	Young's modulus of elasticity
I_x	In-plane second moment of area
k	See Equation 23
L	Length
M	External moment
M_c	Mid-span moment
M_r	Bending moment
N	External axial force
r	Distance of point P(z, y) from flange intersection
r_0	Distance to beam left hand end
$t_{f,w}$	Flange and web thicknesses
v, w	Displacements in y, z directions
V	External shear force
V_f	Sum of vertical components of flange forces
v_P, w_P	Displacements of P(z, y)
x, y	Principal axes
z	Distance along member
α	Flange inclination
ε_r	Strain
θ	Angle from z axis
σ_r	Normal stress in r direction
σ_z	Normal stress in z direction
$\tau_{r\theta}$	Circumferential shear stress
$\tau_{r\theta\alpha}$	Value of $\tau_{r\theta}$ at bottom flange
τ_{0m}, τ_{0n}	See Equation 31
$\tau_{\alpha m}$	See Equation 31

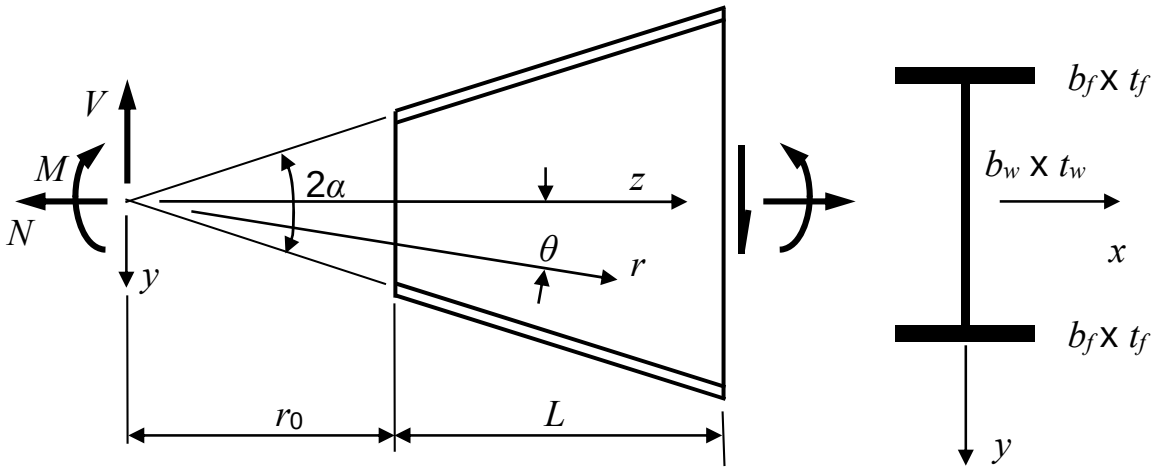

(a) Beam and Loading (b) Section

Fig. 1 Web-Tapered I-Beam

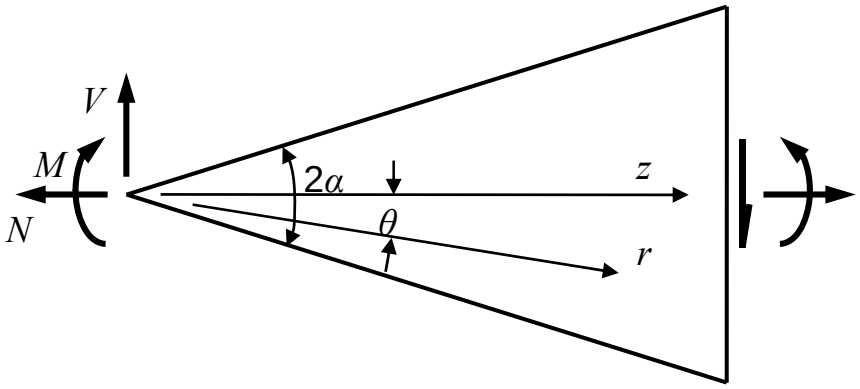

Fig. 2 Wedge

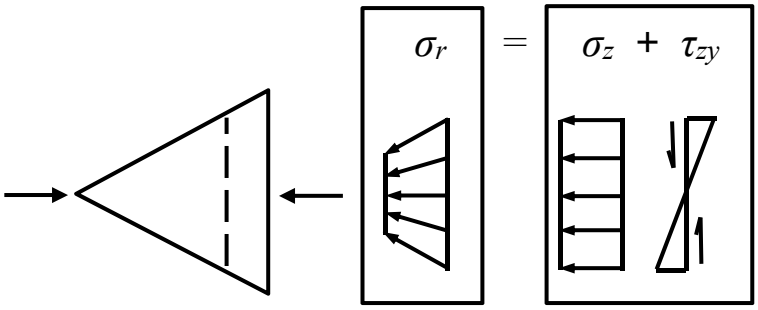

(a) Stresses due to axial force

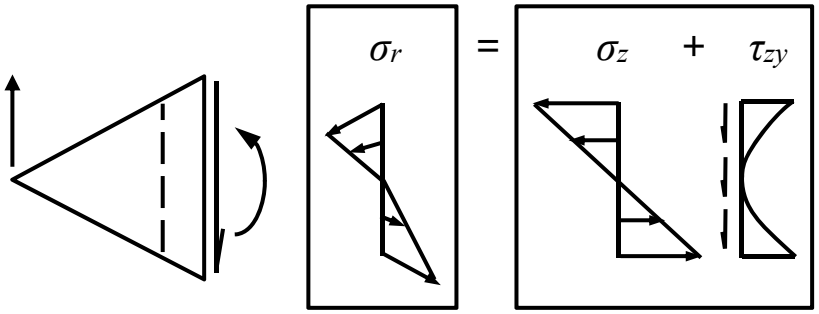

(b) Stresses due to shear

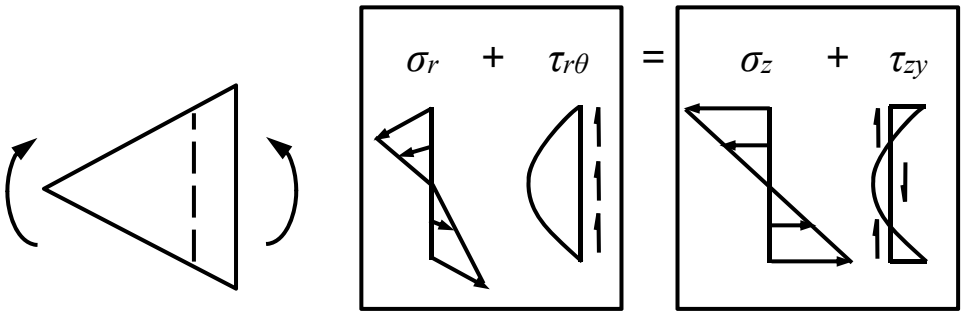

(c) Stresses due to moment

Fig. 3 Mid-Span Stresses in Wedges

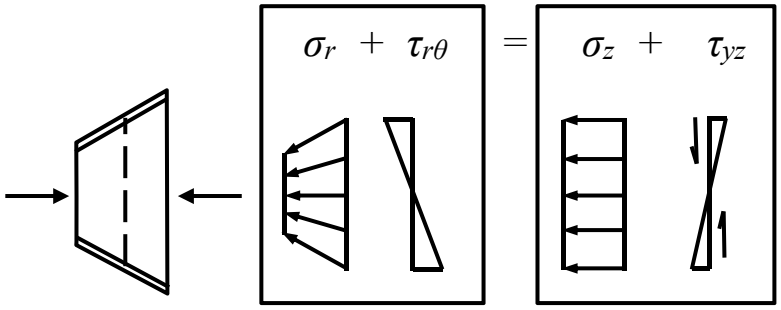

(a) Stresses due to axial force

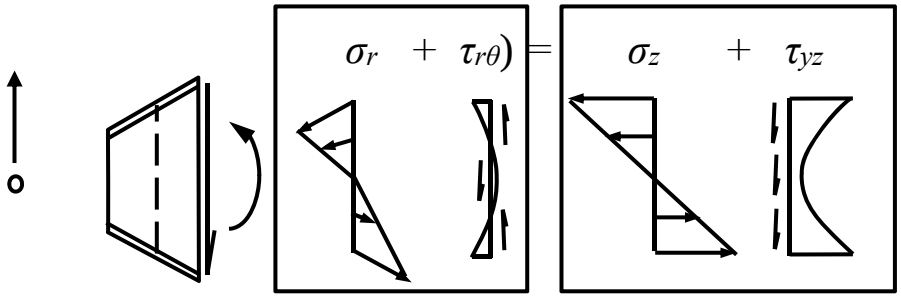

(b) Stresses due to shear

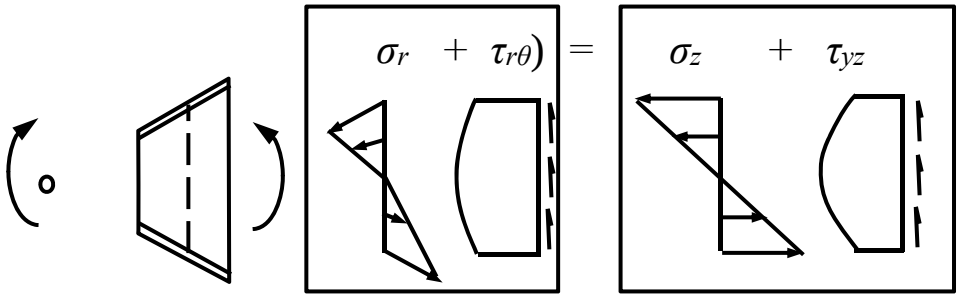

(c) Stresses due to moment

Fig. 4 Mid-Span Stresses in Web-Tapered Beams